Synthesis and applicability of a photolabile 7,7-azi analogue of 3-sulfated taurine-conjugated bile salts

A. Dietrich,* W. Dieminger,* S. Mac Nelly,† W. Gerok,† and G. Kurz[1,]*

Institut für Organische Chemie und Biochemie der Universität Freiburg,* D-79104 Freiburg, Germany, and Medizinische Universitätsklinik Freiburg,† D-79106 Freiburg, Germany

Abstract For the identification of proteins involved in hepatobiliary transport, the photolabile derivative 7,7-ASLCT ((7,7-azi-3α-sulfato-5β-cholan-24-oyl)-2′-aminoethanesulfonate) was synthesized. 7,7-ASLCT is taken up into liver and excreted into bile completely unmetabolized at a rate between the excretion rate of SLCT ((3α-sulfato-5β-cholan-24-oyl)-2′-aminoethanesulfonate) and SCCT ((7α-hydroxy-3α-sulfato-5β-cholan-24-oyl)-2′-aminoethanesulfonate). The dependency of flux rate of uptake into freshly isolated hepatocytes on the concentration of 7,7-ASLCT in presence of Na^+ (143 mM) and with Na^+ depletion (1 mM) is best described by the assumption of two simple transport systems, the kinetic parameters of which are similar to those of SLCT. As studied in the presence of Na^+, 7,7-ASLCT and SLCT exhibit a clearly competitive cross-inhibition of uptake with inhibition constants that are similar to the corresponding half-saturation constants. Photoaffinity labeling of isolated hepatocytes using 7,7-ASLCT (400 μM) resulted in the irreversible inhibition of the uptake of 7,7-ASLCT and SLCT to similar extents, confirming the kinetic data that 7,7-ASLCT is a true competing substrate for the uptake of SLCT. Because in intact rat liver 7,7-ASLCT and SLCT mutually inhibit their biliary excretion, the photolabile derivative shares with SLCT the same pathways in uptake and in excretion. Thus, 7,7-ASLCT should be appropriate for the study of hepatobiliary transport of sulfated and taurine-conjugated bile salts by photoaffinity labeling.–**Dietrich, A., W. Dieminger, S. Mac Nelly, W. Gerok, and G. Kurz.** Synthesis and applicability of a photolabile 7,7-azi analogue of 3-sulfated taurine-conjugated bile salts. *J. Lipid Res.* 1995. **36:** 1729–1744.

Supplementary key words bile salt excretion · bile salt uptake · competing substrates · hepatobiliary transport · Na^+ dependency · photoaffinity labeling

In the course of their enterohepatic circulation taurine- and glycine-conjugated bile salts are subjected to biotransformations by enteral microorganisms (1, 2). Dependent on their structure a substantial part of the microbial modified bile salts is passively resorbed in the colon and reaches the liver with portal blood. They are taken up into the hepatocytes and transformed into more hydrophilic derivatives, the biliary excretion of which is favored (3–5). Unconjugated C_{24} bile salts are reamidated with taurine or glycine and relatively hydrophobic amidated bile salts may be additionally transformed into sulfated derivatives. Sulfation of a hydroxy group introduces an additional charge into the bile salt molecule and increases its hydrophilic character. This way of conjugation is of considerable importance in human bile salt metabolism for the detoxication of hydrophobic amidated bile salts under physiological and pathophysiological conditions (6–10). Excreted into bile the sulfated and amidated bile salts reach the intestine, where they are partly reabsorbed in the terminal ileum (9, 11–13). The intestinal reabsorbed sulfated bile salts are transported back to liver, taken up into the hepatocytes, and returned to enterohepatic circulation. Transport of sulfated and amidated bile salts is of interest because of the application of chenodeoxycholate and ursodeoxycholate for dissolution of cholesterol gallstones (14–16). A part of the administered bile salts is 7-dehydroxylated by intestinal bacteria to lithocholate (2), so that increased levels of sulfated and amidated lithocholic acid in enterohepatic circulation arise from therapy (14). Although sulfation decreases the half-life

Abbreviations: 7,7-ASLCT, 7,7-azi-3α-sulfatolithocholyltaurine or (7,7-azi-3α-sulfato-5β-cholan-24-oyl)-2′-aminoethanesulfonate; [^{3}H]-7,7-ASLCT, 7,7-azi-3α-sulfatolithocholyl[2′-^{3}H(N)]taurine or (7,7-azi-3α-sulfato-5β-cholan-24-oyl)-2′-[2′-^{3}H(N)]aminoethanesulfonate; DCI, direct chemical ionization; EI, electron impact ionization; FAB, fast atom bombardment; HPLC, high performance liquid chromatography; HPTLC, high performance thin-layer chromatography; LSC, liquid scintillation counting; M_r, molecular weight; SCCT, 3α-sulfatochenodeoxycholyltaurine or (7α-hydroxy-3α-sulfato-5β-cholan-24-oyl)-2′-aminoethanesulfonate; [^{3}H]SCCT, 3α-sulfatochenodeoxycholyl[2′-^{3}H(N)]taurine or (7α-hydroxy-3α-sulfato-5β-cholan-24-oyl)-2′-[2′-^{3}H(N)]aminoethanesulfonate; SLCT, 3α-sulfatolithocholyltaurine or (3α-sulfato-5β-cholan-24-oyl)-2′-aminoethanesulfonate; [^{3}H]SLCT, 3α-sulfatolithocholyl[2′-^{3}H(N)]taurine or (3α-sulfato-5β-cholan-24-oyl)-2′-[2′-^{3}H(N)]aminoethanesulfonate; SDS-PAGE, sodium dodecylsulfate polyacrylamide gel electrophoresis; TLC, thin-layer chromatography.

[1]To whom correspondence should be addressed.

time of stay of a bile salt in the organism, sulfated and amidated bile salts may pass through several cycles of enterohepatic circulation (9, 13, 17). Sulfated and non-sulfated bile salts interfere in hepatic transcellular transport (18–20) and it is of interest whether the dianionic sulfated and the monoanionic non-sulfated bile salts interact with the same binding polypeptides in the course of their enterohepatic circulation. Interaction of bile salts with polypeptides under physiological conditions may be favorably detected by photoaffinity labeling using appropriate photolabile derivatives (21, 22). Therefore, we have synthesized a photolabile 7,7-azi analogue of 3α-sulfated taurine-conjugated bile salts and have established its suitability for the identification of hepatic polypeptides interacting with 3α-sulfated taurine-conjugated bile salts during hepatobiliary transport.

MATERIALS AND METHODS

Materials

Cholic acid, silica gel 60 (40–63 μm), and silica gel plates (Kieselgel 60 without fluorescence indicator) for TLC and HPTLC chromatography were purchased from E. Merck (Darmstadt, Germany). Trypan blue and Amberlite XAD-2 (0.3–1 mm particle size, analytical grade) were from Serva Feinbiochemica (Heidelberg, Germany). Taurine was obtained from Sigma Chemie GmbH (Taufkirchen, Germany) and lithocholic acid from Ega-Chemie (Steinheim, Germany). Chenodeoxycholic acid was purchased from Fluka AG (Buchs, Switzerland). Ursodeoxycholic acid was made available by Dr. Falk Pharma GmbH (Freiburg, Germany). Collagenase "Worthington" CLS II with a specific activity of 125–150 U/mg protein was obtained from Biochrom KG (Berlin, Germany). Silicone oils AR 20 and AR 200 were obtained from Wacker Chemie (München, Germany). [2-^{3}H(N)]taurine (750–1500 GBq/mmol) was obtained from NEN/DuPont de Nemours GmbH Division (Dreieich, Germany). All other chemicals were of the highest quality available from commercial sources.

Animals

Male Wistar rats (Tierzuchtanstalt Jautz, Hannover, Germany) weighing 200–250 g were used. The animals had free access to standard rat diet Altromin 300 R (Altromin GmbH, Lage, Germany) and tap water, and were housed in a constant temperature environment with natural day–night rhythm.

Liver infusion experiments

For the study of the time dependency of biliary excretion of sulfated and taurine-conjugated bile salts, amounts of 0.05 nmol of the respective tritium-labeled derivative were dissolved in 0.5 ml of 0.15 M NaCl and infused over a 1-min period into a peripheral mesenterial vein of rats anesthetized with pentobarbital (3 mg of sodium pentobarbital/100 g body weight, i.p.). Bile was collected in 1-min intervals beginning 10 min before start of injection and the nature of the excreted compounds was determined by TLC.

Constant infusion of sulfated and taurine-conjugated bile salts with tracer doses of the respective tritium-labeled derivative was performed as described (23). The rate of infusion was chosen to approximate the maximal rate of bile salt excretion into bile. Forty min after the onset of infusion, animals also received an additional bolus of 0.1 μmol of the second bile salt.

Isolation of hepatocytes

Isolated hepatocytes from rat livers were prepared by a modified collagenase perfusion method using the two-step procedure (24–26) as recently described (22). Only hepatocyte suspensions with an ATP content of > 13.1 nmol/mg protein were used for uptake studies, guaranteeing that only results with cell suspensions having an adequate ATP level were taken into account (27).

Uptake studies and data analyses

Uptake of 7,7-ASLCT and SLCT was determined using the centrifugal filtration technique through silicone oil layer as described (22). Initial rates of uptake were calculated by linear regression analysis from the slope of the linear portion of the time-dependent uptake curves, measured in 15-sec intervals.

Kinetic parameters were analyzed by the nonlinear least-squares regression analysis program ENZFITTER 1.05 (Elsevier-BIOSOFT, Cambridge, UK) in the J-versus-A diagram taking all data into account with the same weight. In general, uptake and inhibition studies were performed five times using a separate preparation of cells for each experiment, and each study was analyzed separately. The resulting kinetic data are reported as means ± SEM. Statistic differences were determined by Student's *t*-test.

Photolysis and photoaffinity labeling

Photolysis and photoaffinity labeling were carried out in a Rayonet RPR 100 reactor (The Southern Ultraviolet Company, Hamden, CT) equipped with 16 RPR 3500 Å lamps. Ultraviolet absorption spectra were measured with a Perkin-Elmer UV/VIS-Spectrometer Lambda 5 (Perkin-Elmer, Überlingen, Germany). Photoaffinity labeling of isolated proteins and protein mixtures was carried out as described (28). The extent of incorporation of radioactivity was determined after SDS-PAGE of defined amounts of labeled proteins, usually 20 or 30

µg, by liquid scintillation counting either directly after electrophoresis or after the staining procedure. For this the gel lanes were cut into slices of 2 mm thickness using a comb for gel slicing. Radioactivity of each gel slice was determined by liquid scintillation counting. Further experimental details of photoaffinity labeling of a mixture of proteins are given in the legend to Fig. 5. Photoaffinity labeling of isolated hepatocytes that were used for uptake studies was performed exactly as described (22).

Polyacrylamide gel electrophoresis

Discontinuous SDS-PAGE using vertical slab gels (200 × 180 × 2.8 mm) was performed as described (29).

Protein determination

Protein concentration was determined after precipitation with 3 M trichloroacetic acid by a modified biuret method (30) using chloroform instead of ether to remove turbidity due to lipid. Bovine serum albumin was used as the standard.

Detection of radioactivity

Radioactivity in organic solvents was determined after addition of 4 ml of Quickszint 501 (Zinsser Analytic GmbH, Frankfurt, Germany) by liquid scintillation counting (RackBeta 1217, Pharmacia LKB, Freiburg, Germany). Radioactivity in aqueous solutions and in bile was determined after addition of 4 ml of Quickszint 1 (Zinsser Analytic GmbH, Frankfurt, Germany). Radioactivity on TLC and HPTLC plates was detected with a radioscanner (Linear Analyzer, Berthold, Wildbad, Germany). Detection of radioactivity in polyacrylamide gels was performed as described (28) using Biolute S (Zinsser Analytic GmbH, Frankfurt, Germany) for solubilization.

Chromatographic methods

TLC and HPTLC were performed on silica gel plates (Kieselgel 60 without fluorescence indicator) using the solvent systems ethyl acetate–cyclohexane–acetic acid 100:40:1 (v/v/v) (solvent system 1), ethyl acetate–cyclohexane–acetic acid 23:7:3 (v/v/v) (solvent system 2), n-butanol–acetic acid–water 9:2:1 (v/v/v) (solvent system 3), and chloroform–methanol–acetic acid–water 65:24:15:9 (v/v/v/v) (solvent system 4). Bile acids and their derivatives were detected on TLC plates by spraying the dried plates with concentrated sulfuric acid and then heating at 120°C for 5 min.

Column chromatography under normal pressure was carried out on 15 × 2.5 cm-columns of Amberlite XAD-2 (31). Flash chromatography (32) was performed on either 25 × 5 cm of 25 × 3 cm-columns of silica gel 60 (40–63 µm).

HPLC of the bile acid *p*-bromophenacyl esters was carried out on an LKB-2150 HPLC-System (Pharmacia-LKB, Freiburg/Germany) equipped with a Rheodyne injector (Cotati, CA) and a single-wavelength (254 nm) UV detector. A reversed-phase µ Bondapack™ C_{18}-column (Waters Associates Inc., Milford, MA), 3.9 mm ID × 300 mm, particle size 5 µm was used with the solvent system methanol–water 78:22 (v/v). The flow rate was 0.7 ml/min at 40°C. HPLC of sulfated and taurine-conjugated bile salts was performed principally as described (33), using the solvent system methanol–10 mM phosphate buffer (pH 5.0) 70:30 (v/v) at ambient temperature with a flow rate of 0.7 ml/min. Radioactivity was detected with a flow-through monitor Ramona 90 (Raytest, Straubenhardt, Germany).

Analysis of organic compounds

Elemental analyses were carried out with a Perkin-Elmer 240 analyzer (Perkin-Elmer GmbH, Überlingen, Germany). Melting points were determined with a Büchi hostage apparatus (Büchi, Flawil, Switzerland) and are uncorrected. Ultraviolet absorption spectra were measured with a Perkin-Elmer UV/VIS-Spectrophotometer Lambda 5 (Perkin-Elmer GmbH, Überlingen, Germany). ^{1}H-NMR spectra were measured on a Bruker-250-MHz-NMR spectrometer (Bruker GmbH, Karlsruhe, Germany). Values are in parts per million relative to tetramethylsilane as internal standard. Mass spectra of unconjugated unsulfated bile salt derivatives were recorded with a Finnigan MAT 44S mass spectrometer connected with a data unit SS 2000 (Finnigan, Sunnyvale, CA). These bile salt derivatives were ionized by EI (electron impact ionization) with an electron energy of 70 eV and by DCI (direct chemical ionization) with an electron energy of 170 eV using ammonia as reactant gas at a pressure of 30 Pa. In both cases positive ions were recorded (34–36). Mass spectra of the sulfated bile salt derivatives were recorded with a VG 70-SE mass spectrometer (VG Instruments Inc., Stanford, CT). The sulfated bile salt derivatives were ionized by bombardment with xenon with an energy acceleration voltage of 8 kV using the FAB (fast atom bombardment) method.

Syntheses

3α-Hydroxy-7-oxo-5β-cholan-24-oic acid (II) (**Fig. 1**). The synthesis of the 7-oxo derivative of lithocholic acid was performed principally according to Fieser and Rajagopalan (37) starting with 5.6 g (14.3 mmol) of chenodeoxycholic acid (I). The crude product was purified by flash chromatography using the solvent system chloroform–methanol 100:1 (v/v). Yield: 2.3 g (5.9 mmol, 41%); mp, 202°C; (Lit.: 202–203°C (37)); TLC: R_f = 0.61 (solvent system 1), 0.25 (solvent system 2); UV (methanol): λ_{max} = 205 nm (ε = 287), 284 nm (ε = 28); ^{1}H-NMR (d_4–MeOH): δ = 0.72 (s, C$\underline{H}_3$–18), 0.97 (d, J = 7 Hz, C$\underline{H}_3$–21), 1.23 (s, C$\underline{H}_3$–19), 2.54 (t, J = 10.5 Hz, C$\underline{H}$–8),

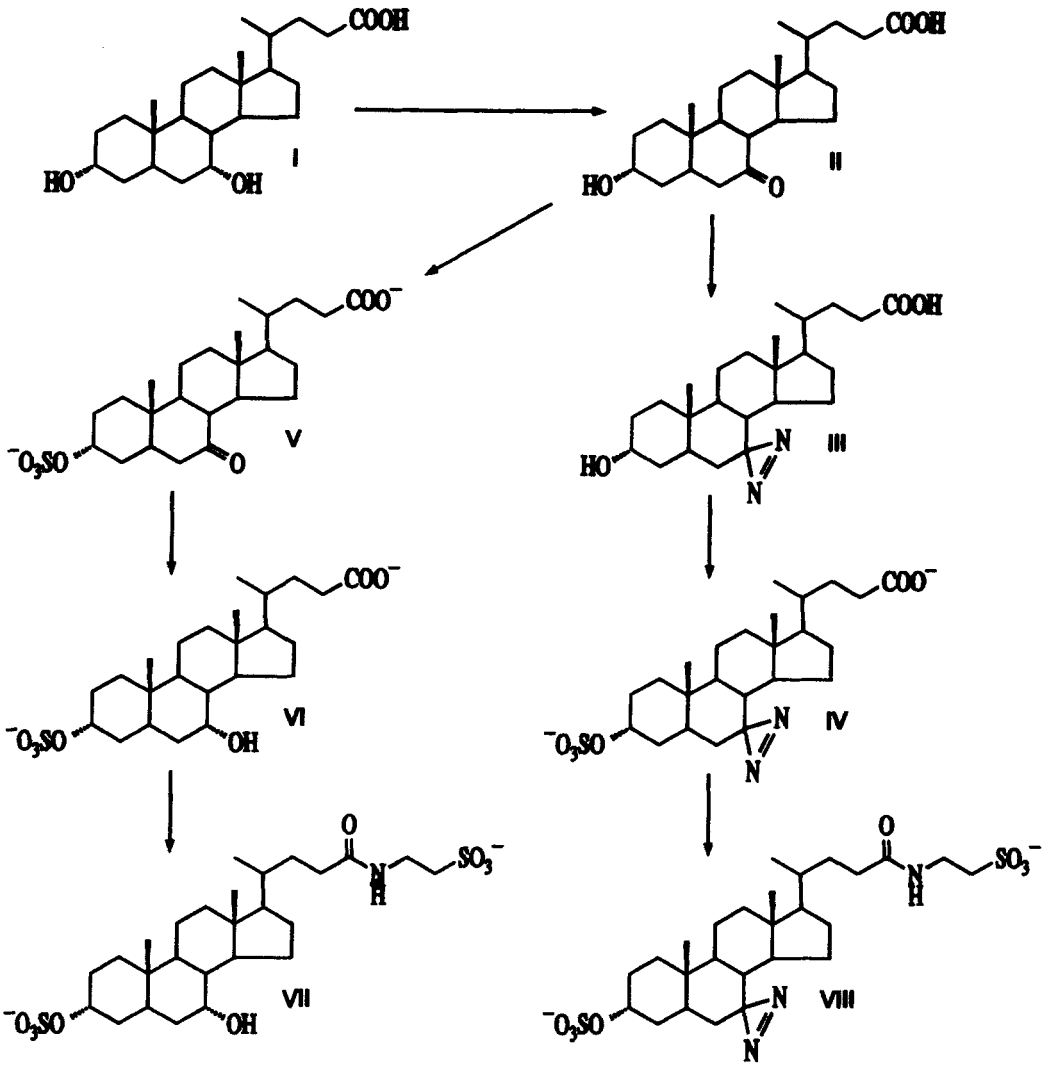

Fig. 1. Synthesis of SCCT ((7α-hydroxy-3α-sulfato-5β-cholan-24-oyl)-2′-aminoethanesulfonate) (VII) and 7,7-ASLCT ((7,7-azi-3α-sulfato-5β-cholan-24-oyl)-2′-aminoethanesulfonate) (VIII). (I), Chenodeoxycholic acid (3α,7α-dihydroxy-5β-cholan-24-oic acid); (II), 3α-hydroxy-7-oxo-5β-cholan-24-oic acid; (III), 7,7-azi-3α-hydroxy-5β-cholan-24-oic acid; (IV), 7,7-azi-3α-sulfato-5β-cholan-24-oate; (V), 7-oxo-3α-sulfato-5β-cholan-24-oate; (VI), 7α-hydroxy-3α-sulfato-5β-cholan-24-oate; (VII), SCCT; (VIII), 7,7-ASLCT.

2.99 (dd, J = 7 and 14 Hz, C$\underline{H}_a$–6), 3.50 (m, C$\underline{H}$–3); mass spectrum (EI): *m/z* = 390 (M^+), 372 (M^+–H_2O), 271 (M^+–H_2O–side chain); anal. calcd. for $C_{24}H_{38}O_4$ (390.6): C, 73.80, H, 9.81; found: C, 73.20, H, 9.75.

7,7-Azi-3α-hydroxy-5β-cholan-24-oic acid (III) (Fig. 1). The 7,7-azi derivative of lithocholic acid was synthesized as described (38) starting with 4 g (9.7 mmol) of 3α-hydroxy-7-oxo-5β-cholan-24-oic acid (II). The crude product was purified by flash chromatography using the solvent system chloroform–methanol 100:2 (v/v). Yield: 2.9 g (7.2 mmol, 74%); mp, 145°C (decomp.); TLC: R_f = 0.42 (solvent system 2), 0.71 (solvent system 3); UV (methanol): λ_{max} = 207 nm (ε = 383), 352 nm (ε = 89), 368 nm (ε = 80); ^{1}H-NMR (d_4–MeOH): δ = 0.63 (s, C$\underline{H}_3$–18), 0.92 (d, J = 7 Hz, CH_3–21), 1.04 (s, CH_3–19), 3.50 (m, C$\underline{H}$–3); mass spectrum (EI): *m/z* = 374 (M^+–N_2), 356 (M^+–N_2–H_2O), 255 (M^+–N_2–H_2O–side chain); mass spectrum (DCI): *m/z* = 420 (M + NH_4^+), 392 (M + NH_4^+–N_2), 374 (M + NH_4^+–N_2–H_2O), 301 (M + NH_4^+–H_2O–side chain); anal. calcd. for $C_{24}H_{38}N_2O_3$ (402.6): C, 71.60, H, 9.51, N, 6.96; found: C, 70.55, H, 9.25, N, 6.42.

Disodium 3α-sulfato-5β-cholan-24-oate, disodium 7,7-azi-3α-sulfato-5β-cholan-24-oate (IV), *and disodium 7-oxo-3α-sulfato-5β-cholan-24-oate* (V) (Fig. 1). Sulfation of the 3α-hydroxy function was performed according to Tserng and Klein (39) with minor modifications. A solution of 8 mmol of the corresponding bile salt derivative and 2.3 g (16.1 mmol) sulfur trioxide–trimethylamine complex in 20 ml of dimethylformamide was stirred overnight at

room temperature. The reaction was stopped by addition of 15 µl of distilled water and the solution was evaporated to about one third of the starting volume. After addition of 200 ml of methanol, containing 0.1 N NaOH, the mixture was stirred for 1 h. Insoluble sodium sulfate was removed by filtration and the residue was washed two times with 3 ml of methanol. The combined filtrates were evaporated to dryness and the residue was freed from traces of nonsulfated starting material and trimethylamine by extracting two times with 30 ml of ether at 0°C. After drying in vacuo, the crude product could be used for synthesis of the taurine conjugates without further purification. For analytical purposes the crude product was dissolved in 50 ml of distilled water and adsorbed on an Amberlite XAD-2 column. The pure product was eluted with methanol and dried in vacuo.

Disodium 3α-sulfato-5β-cholan-24-oate. Yield: 3.4 g (6.9 mmol, 86%); mp, 233°C; (Lit.: 233–235°C (39)); TLC: R_f = 0.13 (solvent system 1), 0.54 (solvent system 3), 0.62 (solvent system 4); UV (methanol): λ_{max} = 208 nm (ε = 750); ^{1}H-NMR (d_4–MeOH): δ = 0.69 (s, C$\underline{H}_3$–18), 0.95 (d, J = 7 Hz, C$\underline{H}_3$–21), 0.95 (s, C$\underline{H}_3$–19), 4.27 (m, C$\underline{H}$–3); mass spectrum (FAB): *m/z* = 501 (M + H^+), 381 (M + H^+–$NaHSO_4$).

Disodium 7,7-azi-3α-sulfato-5β-cholan-24-oate (IV). Yield: 4 g (7.5 mmol), 94%); mp, 188°C (decomp.); TLC: R_f = 0.13 (solvent system 1), 0.54 (solvent system 3), 0.63 (solvent system 4); UV (methanol): λ_{max} = 212 nm (ε = 854), 350 (ε = 82), 368 nm (ε = 80); ^{1}H-NMR (d_4–MeOH): δ = 0.63 (s, C$\underline{H}_3$–18), 0.92 (d, J = 7 Hz, C$\underline{H}_3$–21), 1.04 (s, C$\underline{H}_3$–19), 4.27 (m, C$\underline{H}$–3); mass spectrum (FAB): *m/z* = 527 (M + H^+), 521 (M + Na^+–N_2), 499 (M + H^+–N_2), 407 (M + H^+–$NaHSO_4$), 378 (M + H^+–N_2–$NaHSO_4$), 255 (M^+–N_2–$NaHSO_4$–side chain).

Disodium 7-oxo-3α-sulfato-5β-cholan-24-oate (V). Yield: 3.9 g (7.6 mmol, 97%); mp, 228°C; TLC: R_f = 0.13 (solvent system 1), 0.53 (solvent system 3), 0.55 (solvent system 4); UV (methanol): λ_{max} = 207 nm (ε = 720), 284 nm (ε = 30); ^{1}H-NMR (d_4–MeOH): δ = 0.71 (s, C$\underline{H}_3$–18), 0.96 (d, J = 7 Hz, C$\underline{H}_3$–21), 1.22 (s, C$\underline{H}_3$–19), 4.10 (m, C$\underline{H}$–3); mass spectrum (FAB): *m/z* = 515 (M + H^+), 395 (M + H^+–$NaHSO_4$).

Disodium 7α-hydroxy-3α-sulfato-5β-cholan-24-oate (VI) (Fig. 1). Reduction of the 7-oxo group was principally performed according to Mosbach, Meyer, and Kendall (40). To a solution of 2.3 g (4.6 mmol) of disodium 7-oxo-3α-sulfato-5β-cholan-24-oate (V) in a mixture of 10 ml of dioxane and 25 ml of 0.4 N NaOH 1 g (24.0 mmol) sodium borohydride was added. The reaction mixture was stirred at room temperature for 2 h. Subsequently, the solution was cooled to 0°C and was acidified with 37 ml 1 N HCl, to remove unreacted sodium borohydride. After adjusting the apparent pH value with 2 N NaOH to pH 7, the solution was evaporated to about one third of the starting volume. The crude product was freed from inorganic salts by adsorption chromatography with Amberlite XAD-2 and purified by flash chromatography using the solvent system acetic ester–methanol 100:15 (v/v). The pure product was dried in vacuo. Yield: 1.9 g (3.7 mmol, 80%); mp, 200°C; (Lit.: 197–202°C (41, 42)); TLC: R_f = 0.08 (solvent system 1), 0.52 (solvent system 3), 0.49 (solvent system 4); UV (methanol): λ_{max} = 205 nm (ε = 734); ^{1}H-NMR (d_4–MeOH): δ = 0.68 (s, C$\underline{H}_3$–18), 0.94 (s, C$\underline{H}_3$–19), 0.96 (d, J = 7 Hz, C$\underline{H}_3$–21), 3.76 (m, C$\underline{H}$–7), 4.09 (m, C$\underline{H}$–3); mass spectrum (FAB): *m/z* = 517 (M + H^+), 397 (M + H^+–$NaHSO_4$), 278 (M + Na^+–$NaHSO_4$–H_2O–side chain).

Disodium (3α-sulfato-5β-cholan-24-oyl)-2′-aminoethanesulfonate (SLCT), disodium (7α-hydroxy-3α-sulfato-5β-cholan-24-oyl)-2′-aminoethanesulfonate (SCCT) (VII), *and disodium (7,7-azi-3α-sulfato-5β-cholan-24-oyl)-2′-aminoethanesulfonate (7,7-ASLCT)* (VIII) (Fig. 1). The conjugation of the sulfated bile salt derivatives with taurine was performed via the mixed anhydride method as described (38) starting with 4 mmol of the respective unconjugated bile salt derivative. After stopping the reaction by the addition of 35 ml of distilled water and adjusting the apparent pH value with 6 N HCl to pH 2, the unconjugated bile salt was extracted three times with 50 ml of ethyl acetate each. The taurine-conjugated bile salt was separated by adsorption on an Amberlite XAD-2 column. The adsorbed derivative was eluted with methanol and the eluate was evaporated to dryness. After dissolving the residue in 25 ml of methanol containing 0.4 N NaOH, the crude product was precipitated by adding 50 ml of ether and stirring the resulting suspension for 1 h at 0°C. The precipitate was filtered off, washed two times with 10 ml of a mixture of methanol–ether 1:5 (v/v) and subsequently two times with ether. The product was dried in vacuo.

Disodium (3α-sulfato-5β-cholan-24-oyl)-2′-aminoethanesulfonate (SLCT). Yield: 1.4 g (2.3 mmol, 57%); mp, 214°C (decomp.); (Lit.: 212–214°C (39)); TLC: R_f = 0.26 (solvent system 3), 0.25 (solvent system 4); UV (methanol): λ_{max} = 207 nm (ε = 709); ^{1}H-NMR (d_4–MeOH): δ = 0.69 (s, C$\underline{H}_3$–18), 0.95 (s, C$\underline{H}_3$–19), 0.97 (d, J = 7 Hz, C$\underline{H}_3$–21), 2.95 (t, J = 7 Hz, C$\underline{H}_2$–2′), 3.57 (t, J = 7 Hz, C$\underline{H}_2$–1′), 4.27 (m, C$\underline{H}$-3); mass spectrum (FAB): *m/z* = 652 (M + 2Na^+–H^+), 630 (M + Na^+), 510 (M + Na^+–$NaHSO_4$), 280 (M + Na^+–$NaHSO_4$–side chain), 165 ($Na_3SO_4^+$), 143 ($Na_2HSO_4^+$).

Disodium (7a-hydroxy-3α-sulfato-5β-cholan-24-oyl)-2′-aminoethanesulfonate (SCCT) (VII). Yield: 1.3 g (2.1 mmol, 52%); mp, 183°C (decomp.); (Lit.: 183–184°C (42)); TLC: R_f = 0.19 (solvent system 3), 0.17 (solvent system 4); UV (methanol): λ_{max} = 207 nm (ε = 622); ^{1}H-NMR (d_4–MeOH): δ = 0.66 (s, C$\underline{H}_3$–18), 0.91 (s, C$\underline{H}_3$–19), 0.94 (d, J = 7 Hz, C$\underline{H}_3$–21), 2.94 (t, J = 7 Hz,

CH_2–2′), 3.56 (t, J = 7 Hz, CH_2–1′), 3.78 (m, CH–7), 4.12 (m, CH–3); mass spectrum (FAB): *m/z* = 668 (M + $2Na^+$–H), 646 (M + Na^+), 526 (M + Na^+–$NaHSO_4$), 278 (M + Na^+–$NaHSO_4$–H_2O–side chain).

Disodium (7,7-azi-3α-sulfato-5β-cholan-24-oyl)-2′-aminoethanesulfonate (7,7-ASLCT) (VIII). Yield: 1.4 g (2.2 mmol, 54%); mp, 201°C (decomp.); TLC: R_f = 0.26 (solvent system 3), 0.25 (solvent system 4); UV (methanol): λ_{max} = 210 nm (ε = 865), 350 nm (ε = 80), 368 nm (ε = 72); ^{1}H-NMR (d_4–MeOH): δ = 0.63 (s, CH_3–18), 0.92 (d, J = 7 Hz, CH_3–21), 1.05 (s, CH_3–19), 2.94 (t, J = 7 Hz, CH_2–2′), 3.56 (t, J = 7 Hz, CH_2–1′), 4.23 (m, CH–3); mass spectrum (FAB): *m/z* = 628 (M + Na^+–N_2), 508 (M + Na^+–N_2–$NaHSO_4$), 278 (M + Na^+–N_2–$NaHSO_4$–side chain).

Synthesis of radioactively labeled bile salt derivatives

Conjugation of cholic acid, 7,7-azi-3α-hydroxy-5β-cholan-24-oic acid and of the sulfated bile salt derivatives with [2-^{3}H(N)]taurine was carried out as described (38). The radiochemical yields of pure products were 4.6 MBq (50%) having a specific activity of 750–1500 Bq/mmol. In order to reduce radiolytic decomposition the products were dissolved in dry methanol (1 Bq/μl) and the solutions were kept in the dark at −20°C.

Determination of the ratio of diastereomeric 7-hydroxy bile salts

In order to determine the product ratio of reduction of 3α-sulfato-7-oxo-5β-cholan-24-oate (V) by $NaBH_4$, desulfation of the 3α-sulfato function was carried out by methanolysis (43). The resulting methyl esters of 3α,7ξ-dihydroxy-5β-cholan-24-oic acid were hydrolyzed with lithium hydroxide in aqueous methanol (44). The *p*-bromophenacyl esters of the resulting diastereomeric bile salt mixture and of the respective reference bile salts were synthesized as described (45).

RESULTS AND DISCUSSION

Syntheses

SCCT (VII) and 7,7-ASLCT (VIII) were synthesized starting from chenodeoxycholic acid (I), which has with the 3α- and the 7α-hydroxy group appropriate functional groups, allowing a convenient synthesis of both derivatives from the common intermediate product 3α-hydroxy-7-oxo-5β-cholan-24-oic acid (II). The 7-oxo intermediate, easily obtained by selective oxidation with N-bromosuccinimide (1, 38, 46), is necessary for the introduction of the 7,7-azi group and allows the synthesis of the 7α-hydroxy-3α-sulfato-5β-cholan-24-oate (VI) without the need of a protecting group for the 7-hydroxy group. Sulfation of both, 3α-hydroxy-7-oxo-5β-cholan-24-oic acid (II) and 7,7-azi-3α-hydroxy-5β-cholan-24-oic acid (III), occurs in high yields practically without the formation of by-products.

Reduction of 7-oxo derivatives of 3α-hydroxy bile salts results predominantly in the formation of the desired 7α-hydroxy derivatives (38, 40, 46). In order to determine the influence of the 3α-sulfato group on the ratio of diastereomers formed by reduction of the 7-oxo-3α-sulfato-5β-cholan-24-oate (V) with sodium borohydride, the reduction products were desulfated by acidic methanolysis (43). The resulting methyl esters were hydrolyzed with lithium hydroxide and the free acids were transformed to their *p*-bromophenacyl esters (44, 45). Separation of the 7α- and 7β-derivatives by HPLC and comparison with the *p*-bromophenacyl esters of the authentic chenodeoxycholic and ursodeoxycholic acids showed (**Fig. 2**) that the reduction of 7-oxo-3α-sulfato-5β-cholan-24-oate (V) with sodium borohydride results in a diastereomeric ratio of 7α-hydroxy- to 7β-hydroxy-derivative of about 95:5. The taurine conjugates (VII and VIII) of the synthesized bile salt derivatives and the tritium-labeled derivatives were obtained in convenient yields by the mixed anhydride method (38).

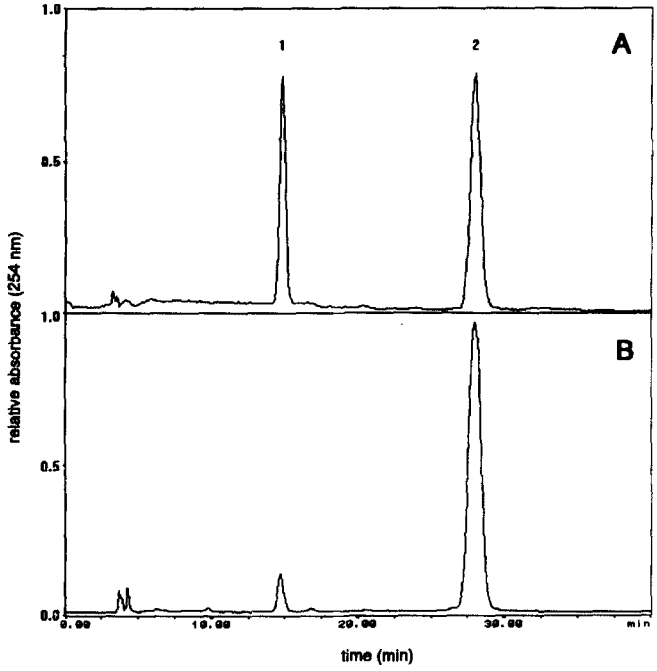

Fig. 2. Determination of the ratio of diastereomers formed by reduction of 7-oxo-3α-sulfato-5β-cholan-24-oate with $NaBH_4$. After desulfation, 3α, 7ξ-dihydroxy-5β-cholanoic-24-acid was transformed to their *p*-bromophenacyl esters and the resulting mixture was analyzed by HPLC. A: *p*-Bromophenacyl esters of authentic 3α,7β-dihydroxy-5β-cholanoic-24-acid (1) and of 3α,7α-dihydroxy-5β-cholanoic-24-acid (2). B: Diastereomers formed by reduction of 7-oxo-3α-sulfato-5β-cholan-24-oate.

Photolysis and suitability for photoaffinity labeling

7,7-ASLCT, like other 7,7-azi derivatives of bile salts and their metabolic precursors (38, 46), exhibits an absorption maximum at 350 nm and a second maximum at 366 nm. Photolysis of 7,7-ASLCT with a light source having its maximum of ultraviolet radiation at 350 nm followed, under the experimental conditions used, first order kinetics with a half-life time of 1.4 min (**Fig. 3**). In order to evaluate the suitability of 7,7-ASLCT for the identification of binding polypeptides, rat serum albumin was subjected to photoaffinity labeling. The amount of radioactivity covalently bound to albumin increased with irradiation time during the first 5 min (**Fig. 4**), yielding a half-life time of incorporation of 1.5 min. Under the experimental conditions used, about 5% of the photolabile derivative was incorporated covalently into albumin. To examine the relative specifity of the labeling process (47), rat serum albumin was subjected to photoaffinity labeling in the presence of equal amounts of other proteins. As demonstrated by SDS-PAGE of the protein mixture used (**Fig. 5A**), incorporation of radioactivity occurred only in albumin (Fig. 5B).

Uptake of 7,7-ASLCT and SLCT into freshly isolated hepatocytes

In order to ensure the applicability of the photolabile derivative 7,7-ASLCT as a model compound for the study of hepatobiliary transport of SLCT, convincing evidence must be provided that the photolabile derivative is transported by the same transport systems and

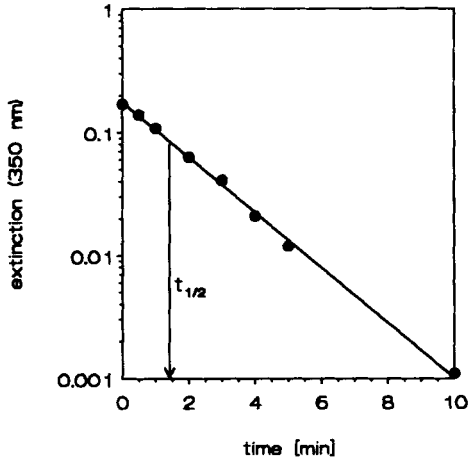

Fig. 3. Determination of the half-life time of the azi group during photolysis of 7,7-ASLCT. A 2.44 mM solution of 7,7-ASLCT in a medium consisting of 118 mM NaCl, 4.74 mM KCl, 1.2 mM $MgCl_2$, 0.59 mM KH_2PO_4, 0.59 mM Na_2HPO_4, 24 mM $NaHCO_3$, and 5.5 mM D-glucose, saturated with carbogen (95% O_2/5% CO_2) and adjusted to pH 7.4, was photolyzed for the times indicated with light having a maximum at 350 nm. The absorbance of 7,7-ASLCT was determined after the illumination time given. The decrease of the extinction at 350 nm is directly proportional to photolyzed 7,7-ASLCT.

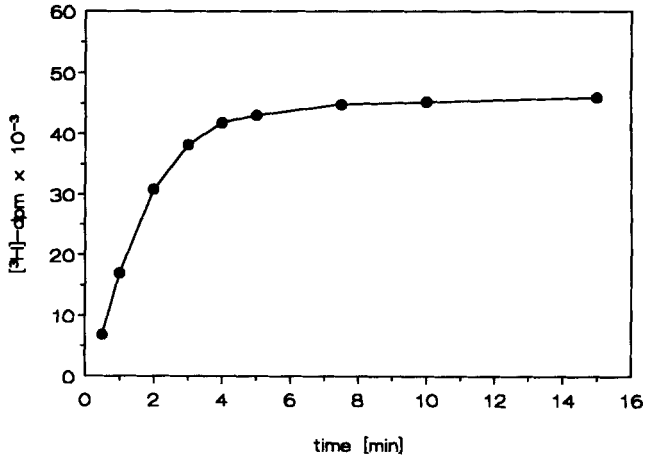

Fig. 4. Photoaffinity labeling of rat serum albumin by [^{3}H]-7,7-ASLCT. A solution of 2 µM rat serum albumin and 0.4 µM [^{3}H]-7,7-ASLCT in 0.1 M sodium phosphate buffer, pH 7.4, was irradiated for the times indicated at 350 nm after 10 min of incubation at 37°C. Incorporation of radioactivity into albumin was estimated after SDS-PAGE by determination of the radioactivity in 2-mm slices of the corresponding gel lanes by liquid scintillation counting.

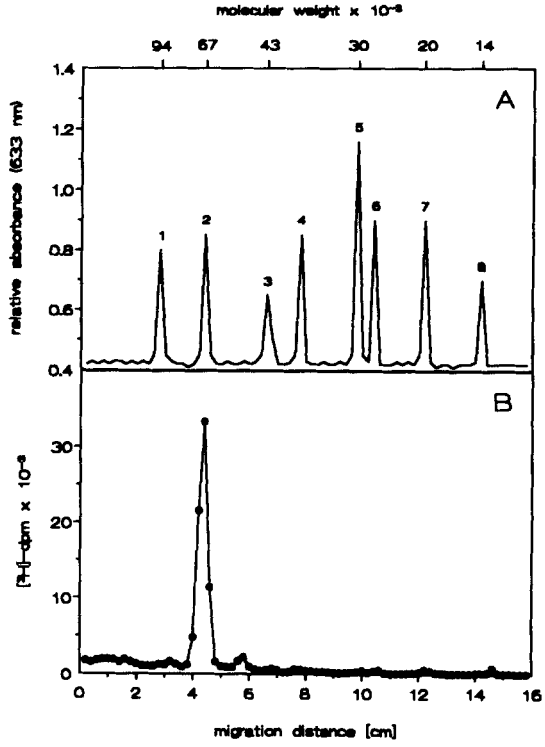

Fig. 5. Photoaffinity labeling of a mixture of purified proteins (each 100 µg) by [^{3}H]-7,7-ASLCT. 1, Phosphorylase b; 2, bovine serum albumin; 3, ovalbumin from chicken egg; 4, glycerol aldehyde-3-phosphate dehydrogenase from rabbit muscle; 5, carbonic anhydrase from bovine erythrocytes; 6, trypsinogen from bovine pancreas; 7, trypsin inhibitor from soybean; 8, α-lactalbumin from bovine milk, and 1.4 µM (500 kBq) [^{3}H]-7,7-ASLCT dissolved in 400 µl of 0.1 M sodium phosphate buffer, pH 7.4, were irradiated at 350 nm for 10 min. In the represented experiment the concentration of bovine serum albumin was 3.73 µM and that of 7,7-ASLCT was 1.4 µM. Incorporation of radioactivity into proteins was estimated after SDS-PAGE by determination of radioactivity in 2-mm slices of the corresponding gel lanes by liquid scintillation counting. A: Distribution of proteins. B: Incorporation of radioactivity.

mechanisms as the physiological compound. Therefore, the uptake of 7,7-ASLCT into freshly isolated hepatocytes was studied in the concentration range from 1 μM to 500 μM and compared with that of SLCT. Because the uptake of different bile salts into hepatocytes exhibits a different dependency on the extracellular concentration of Na^+ (22), these comparative studies were performed in the presence of a Na^+ concentration in the physiological range (143 mM) and in a medium depleted of Na^+ (1 mM).

The dependency of initial influx rates on the extracellular concentration of 7,7-ASLCT exhibited saturability in the presence of Na^+ and in the case of Na^+ depletion (**Fig. 6A**). In comparison to the uptake in the presence of a physiological concentration of Na^+, in the case of Na^+ depletion transport of 7,7-ASLCT is decreased by about 45%. The effect of extracellular Na^+ on the uptake of 7,7-ASLCT is not so strong as with cholyltaurine for which the decrease amounts to about 75% (22).

Monoanionic taurine-conjugated as well as unconjugated bile salts are taken up into isolated rat hepatocytes by two distinct transport systems and show, therefore, a complex dependency of initial uptake rate on extracellular bile salt concentration (22, 48). In order to analyze whether the dependency of uptake rate on the concentration of 7,7-ASLCT (Fig. 6A) follows the kinetic mechanism for a simple carrier-mediated transport or whether a more complex mechanism has to be taken into account, as for the monoanionic bile salts, the initial influx rates were plotted using the J/A-versus-J plot (Fig. 6B). The graphs demonstrate that the data obtained with Na^+ depletion fit a curve that clearly deviates from linearity, whereas the data obtained in the presence of Na^+ fit a curve that deviates only very slightly from linearity, provided that that is the case at all. This excludes that the uptake of 7,7-ASLCT into isolated hepatocytes may be described by the equation for one simple transport process and suggests as the simplest kinetic assumption that two different transport systems with a different dependency on the concentration of Na^+ are operative in parallel, exactly as demonstrated for the uptake of monoanionic bile salts (22, 48). Thus, total uptake of 7,7-ASLCT may be described by flux equation 1:

$$J_{total} \approx \frac{J_1 \cdot A}{K_{T1}+A} + \frac{J_2 \cdot A}{K_{T2}+A} \qquad \textit{Eq. 1)}$$

The symbols used are defined in **Table 1.**

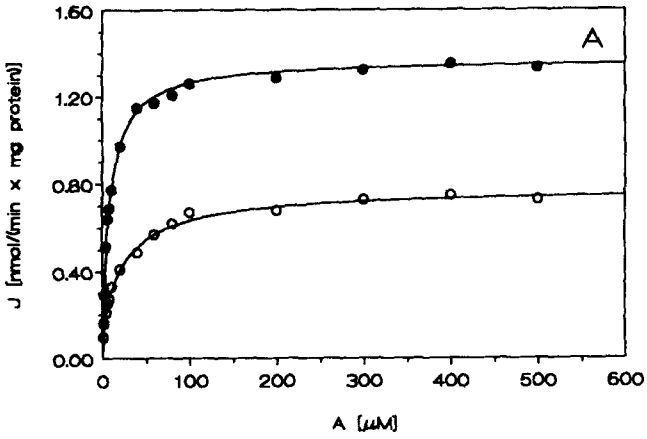

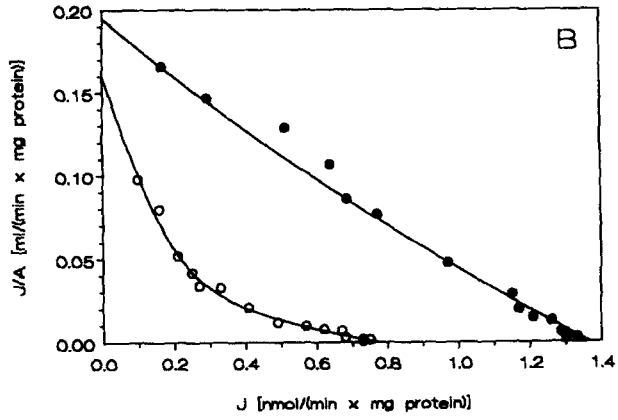

Fig. 6. Dependency of initial flux rates of 7,7-ASLCT into freshly isolated hepatocytes on 7,7-ASLCT concentration; (●) in the presence of 143 mM Na^+ (standard medium) and (○) in the presence of 1 mM Na^+ (Na^+-depleted medium). A: J-versus-A plot, B: J/A-versus-J plot. The points represent the data of typical experiments; curves were calculated applying equation 1 with the kinetic parameters evaluated for uptake of 7,7-ASLCT.

TABLE 1. List of symbols and definitions

Symbol	Definition	Unit
A	Concentration of substrate	μM
I	Concentration of inhibitor	μM
J_{total}	Maximal total flux rate	nmol/(min · mg protein)
J_1	Maximal flux rate of transport system 1	nmol/(min · mg protein)
J_2	Maximal flux rate of transport system 2	nmol/(min · mg protein)
K_T	Half-saturation constant	μM
K_{T1}	Half-saturation constant of transport system 1	μM
K_{T2}	Half-saturation constant of transport system 2	μM
K_I	Inhibition constant of transport	μM
K_{I1}	Inhibition constant of transport system 1	μM
K_{I2}	Inhibition constant of transport system 2	μM

Subscripts added in parentheses give Na^+ concentration under the experimental conditions. The subscript *app* denotes apparent K_T values obtained in the presence of an inhibitor. For the competing substrate A′ symbols are indicated by a prime.

Whereas the data obtained in the presence of Na^+ do not allow an unambiguous analysis, those obtained with Na^+ depletion render possible a reliable graphical analysis for the subsequent calculation of the kinetic parameters by nonlinear regression analysis. The kinetic parameters for the assumed two transport systems in case of Na^+ depletion are:

$J_{1(Na^+\,1)}$ = 0.20 ± 0.04 nmol / (min · mg protein)

$K_{T1(Na^+\,1)}$ = 1.40 ± 0.3 μM

$J_{2(Na^+\,1)}$ = 0.59± 0.06 nmol / (min · mg protein)

$K_{T2(Na^+\,1)}$ = 33.0 ± 4.5 μM

In order to analyze the dependency of initial influx rates in the presence of Na^+ on the concentration of 7,7-ASLCT, use was made of the inhibition of 7,7-ASLCT uptake by cholyltaurine. The inhibitory effect of cholyltaurine on the initial flux rates of 7,7-ASLCT in the presence of Na^+ is shown in the J-versus-A plot (**Fig. 7A**). The linear transformation of the kinetic data in the J/A-versus-J plot (Fig. 7B) demonstrates that the different curves intersect the abscissa at one single point. This indicates that cholyltaurine acts as a competitive inhibitor for the uptake of 7,7-ASLCT.

In contrast to the curve resulting in the J/A-versus-J plot from the data of 7,7-ASLCT uptake in the absence of the inhibitor, the curves with the data obtained in the presence of cholyltaurine exhibit a clear deviation from linearity (Fig. 7B). This allows the calculation of the kinetic parameters of the inhibited 7,7-ASLCT uptake by the two assumed transport systems (**Table 2**). As to be expected for a competitive inhibition, the kinetic parameters demonstrate that the maximal flux rates of 7,7-ASLCT uptake by the two transport systems remain unchanged with increasing inhibitor concentration. These two maximal flux rates must be identical with those for the 7,7-ASLCT uptake in absence of any inhibitor. Only the apparent half-saturation constants K_{T1app} and K_{T2app} for 7,7-ASLCT are increased by increasing concentrations of cholyltaurine, that for transport system 1 only slightly but that for transport system 2 clearly.

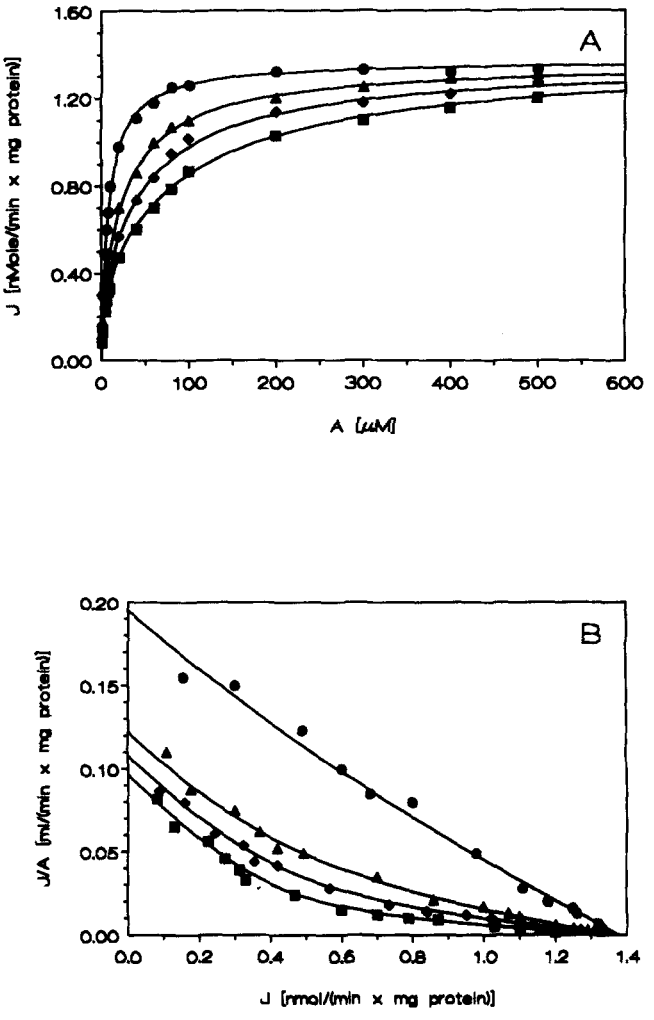

Fig. 7. Effect of different concentrations of cholyltaurine on the dependency of initial flux rates of 7,7-ASLCT into isolated hepatocytes on 7,7-ASLCT concentration in presence of 143 mM Na^+ (standard medium); (●) in the absence of cholyltaurine, and in the presence of 50 μM (▲), 100 μM (◆), 200 μM (■) cholyltaurine. A: J-versus-A plot, B: J/A-versus-J plot. The points represent the data of a typical experiment. Curves were calculated applying equation 1, using for the inhibitions with cholyltaurine the maximal flux rates and apparent half-saturation constants obtained as the means of five determinations, and for the uninhibited case the kinetic parameters evaluated for the uptake of 7,7-ASLCT.

TABLE 2. Effect of the presence of cholyltaurine on the kinetic parameters of uptake of 7,7-ASLCT

	Transport System 1		Transport System 2	
Cholyltaurine	K_{T1app}	J_1	K_{T2app}	J_2
μM	μM	*nmol/(min • mg protein)*	μM	*nmol/(min • mg protein)*
50	3.9 ± 0.6	0.36 ± 0.04	32.8 ± 4.7	1.00 ± 0.06
100	4.2 ± 0.6	0.38 ± 0.04	59.0 ± 5.1	0.98 ± 0.06
200	4.7 ± 0.7	0.38 ± 0.03	104.3 ± 9.0	1.00 ± 0.06

This demonstrates that cholyltaurine predominantly inhibits the uptake of 7,7-ASLCT by transport system 2. For a pure competitive system the $K_{T_{app}}$ is a linear function of the inhibitor concentration as described by equation 2:

$$K_{T_{app}} = K_T + \frac{K_T}{K_I} \bullet I \qquad \textit{Eq. 2)}$$

which allows the estimation of both K_T and K_I. Due to the relatively high experimental error the inhibition of transport system 1 was not sufficient for a useful determination of the corresponding kinetic constants, whereas the inhibition of transport system 2 allowed the estimation of K_{T2} and K_{I2}. The estimated half-saturation constant of transport system 2 is: K_{T2} = 10.2 ± 3 μM and the corresponding inhibition constant of cholyltaurine is: K_{I2} = 22.0 ± 7.3 μM.

With the kinetic parameters J_1, J_2, and K_{T2}, derived from 7,7-ASLCT uptake in the presence of Na^+ using cholyltaurine as an inhibitor, the value of K_{T1} could be calculated from the uninhibited uptake of 7,7-ASLCT by regression analysis using equation 1 as a basis. For the uptake of 7,7-ASLCT in the presence of Na^+ the estimated K_{T1} value is K_{T1} = 3.6 ± 1 μM.

Under the experimental conditions, it is difficult to obtain accurate measurements of initial influx rates at sufficiently low 7,7-SLCT concentrations. Therefore, evaluation of the inhibition constant of cholyltaurine for the uptake of 7,7-ASLCT by transport system 1, contributing less than transport system 2 to total uptake rate, was not possible with the necessary reliability. The inhibition is so low that even at relative high cholyltaurine concentrations the experimental data contain little useful information.

Uptake of SLCT was compared to determine whether the introduction of the azi group resulted in a changed behavior in hepatic transport of the physiological compound. As with the photolabile derivative, the dependency of the initial influx rates on the concentration of SLCT showed in the presence of Na^+ and with Na^+ depletion saturability (**Fig. 8A**). Na^+ depletion resulted in a decrease of the total maximal influx rate of about 55%, which is in the same range as with the photolabile derivative. As with 7,7-ASLCT, the data obtained with Na^+ depletion allowed the calculation of the kinetic parameters for two transport systems inferred from the J/A-versus-J plot (Fig. 8B). The calculated kinetic parameters are:

$J'_{1(Na^+\,1)}$ = 0.25 ± 0.03 nmol / (min · mg protein)

$K'_{T1(Na^+\,1)}$ = 1.50 ± 0.3 μM

$J'_{2(Na^+\,1)}$ = 0.59± 0.056 nmol / (min · mg protein)

$K'_{T2(Na^+\,1)}$ = 36.8 ± 3.9 μM

A detailed kinetic analysis of the dependency of initial influx rates in the presence of Na^+ on the concentration of SLCT and of their inhibition by cholyltaurine (**Fig. 9**) demonstrated that the inhibition is clearly a competitive one (Fig. 9B) and allowed the calculation of the maximal velocities of the two assumed transport systems and of the apparent half-saturation constants in the presence of the inhibitor (**Table 3**). Using the correlation described by equation 2, the half-saturation constant of transport system 2 for SLCT and the corresponding inhibition constant for cholyltaurine were estimated at: K'_{T2} = 11.4 ± 2 μM and K'_{I2} = 21.0 ± 4.2 μM.

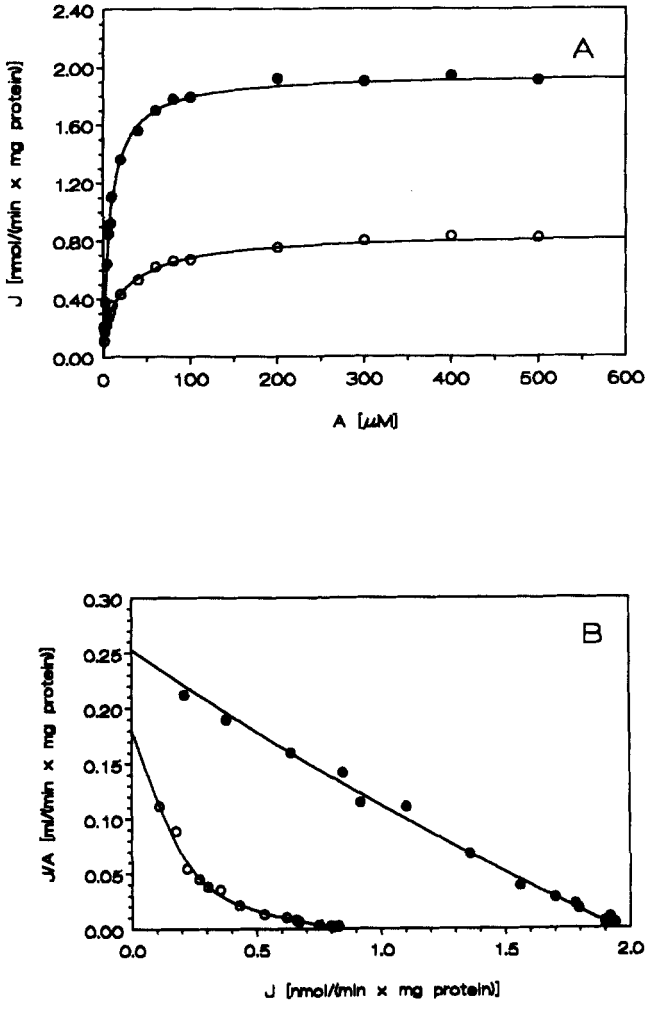

Fig. 8. Dependency of initial flux rates of SLCT into freshly isolated hepatocytes on SLCT concentration; (●) in the presence of 143 mM Na^+ (standard medium) and (○) in the presence of 1 mM Na^+ (Na^+-depleted medium). A: J-versus-A plot, B: J/A-versus-J plot. The points represent the data of typical experiments. Curves were calculated applying equation 1 with the kinetic parameters evaluated for uptake of SLCT.

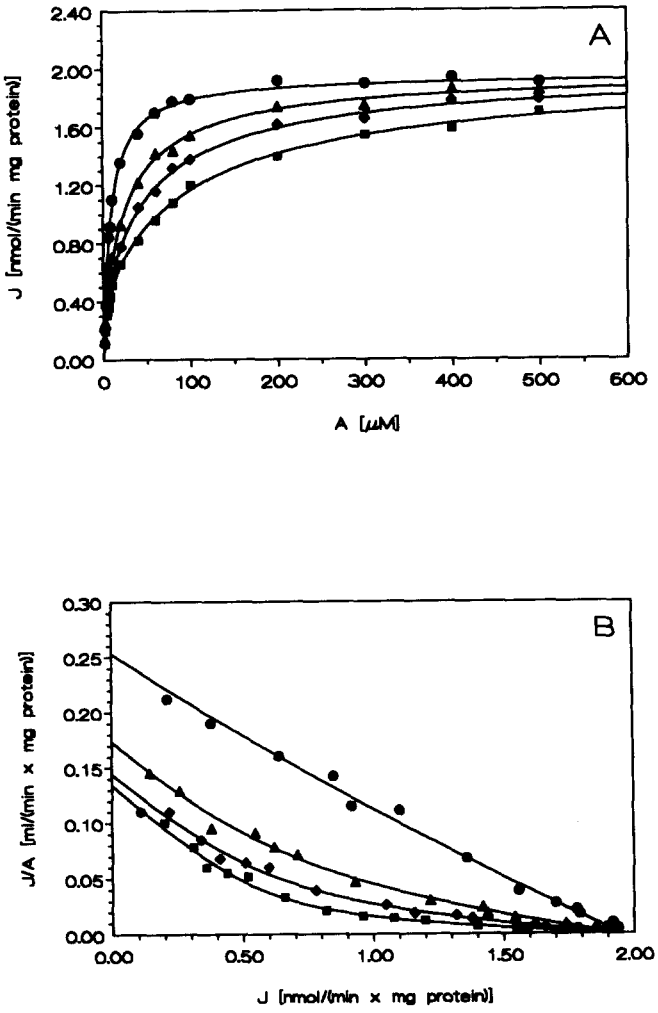

Fig. 9. Effect of different concentrations of cholyltaurine on the dependency of initial flux rates of SLCT into isolated hepatocytes on SLCT concentration in presence of 143 mM Na^+ (standard medium); (●) in the absence of cholyltaurine, and in the presence of 50 μM (▲), 100 μM (◆), 200 μM (■) cholyltaurine. A: J-versus-A plot, B: J/A-versus-J plot. The points represent the data of a typical experiment. Curves were calculated applying equation 1, using for the inhibitions with cholyltaurine the maximal flux rates and apparent half-saturation constants obtained as the means of five determinations, and for the uninhibited case the kinetic parameters evaluated for the uptake of SLCT.

With the kinetic parameters J'_1, J'_2, and K'_{T2}, derived from the inhibition of SLCT uptake in the presence of Na^+ by cholyltaurine, K'_{T1} was calculated from the data obtained for SLCT uptake in the absence of the inhibitor by nonlinear regression analysis to be: $K'_{T1} = 3.9 \pm 1.3$ μM.

As with 7,7-ASLCT, the experimental error was too high for a useful estimation of the inhibition constant of transport system 1. Due to the relative high variation of the experimental data, the numerical values of the estimated kinetic constants may mean little, but they allow us to draw the conclusion that with regard to its uptake into isolated hepatocytes 7,7-ASLCT behaves comparably to the physiological compound SLCT. Both sulfated and taurine-conjugated bile salts are taken up by two different transport systems and the one exhibiting the higher half-saturation constants for both sulfated bile salts is inhibited by cholyltaurine with nearly the same effectivity.

Cross inhibition of uptake of 7,7-ASLCT and SLCT

Having estimated the kinetic parameters for the uptake of 7,7-ASLCT and SLCT into freshly isolated hepatocytes, it has been possible to diagnose whether the photolabile derivative is a true alternative substrate of SLCT. The velocity equation 3 for two transport systems catalyzing the uptake of the same substrate in the presence of an alternative substrate

$$J_{total} = \frac{J_1 \bullet A}{K_{T1} \bullet (1 + \frac{A'}{K'_{T1}}) + A} + \frac{J_2 \bullet A}{K_{T2} \bullet (1 + \frac{A'}{K'_{T2}}) + A} \qquad \textit{Eq. 3)}$$

demonstrates that the alternative substrate has the same effect as a strictly competitive inhibitor with inhibition constants that are equal to the half-saturation constants of the alternative substrate. In the reverse case, likewise, a strictly competitive inhibition with the identity of the inhibition constants and the corresponding half-saturation constants must be observed.

Thus, it is possible to examine whether 7,7-ASLCT and SLCT exhibit a competitive cross-inhibition of their uptake into isolated hepatocytes and to consider whether the estimated kinetic constants are reasonable. The inhibitory effect of appropriate fixed concentra-

TABLE 3. Effect of the presence of cholyltaurine on the kinetic parameters of uptake of SLCT

	Transport System 1		Transport System 2	
Cholyltaurine	K'_{T1app}	J'_1	K'_{T2app}	J'_2
μM	μM	*nmol/(min · mg protein)*	μM	*nmol/(min · mg protein)*
50	4.0 ± 0.6	0.55 ± 0.03	39.2 ± 3.1	1.40 ± 0.03
100	4.8 ± 0.6	0.56 ± 0.04	64.0 ± 5.1	1.40 ± 0.04
200	4.4 ± 0.6	0.55 ± 0.03	119.7 ± 7.5	1.38 ± 0.04

tions of SLCT on the dependency of initial flux rates on the concentration of 7,7-ASLCT in the presence of Na^+ is shown in the J-versus-A plot (**Fig. 10A**). The type of inhibition becomes obvious in the J/A-versus-J plot (Fig. 10B), where all curves intersect at a common point on the abscissa. Whereas the total maximal flux rate of 7,7-ASLCT uptake remained constant, the apparent K_T values are affected by SLCT, indicating that it behaves as a competitive inhibitor. In the reverse case, for the inhibition of uptake of SLCT by 7,7-ASLCT (**Fig. 11A**), likewise, a clear competitive inhibition was observed, as shown in the J/A-versus-J plot (Fig. 11B).

7,7-ASLCT and SLCT exhibit a strictly competitive cross-inhibition of uptake into freshly isolated hepatocytes with inhibition constants comparable to the half-saturation constants of uptake of the respective alternative substrate, as demonstrated by the relatively good fit of the experimental data to the curves obtained with the kinetic parameters determined for both substrates assuming two distinct transport systems. This kinetic behavior is a strong argument for the involvement of the same two transport systems in the uptake of the photolabile derivative 7,7-ASLCT and the physiological compound SLCT.

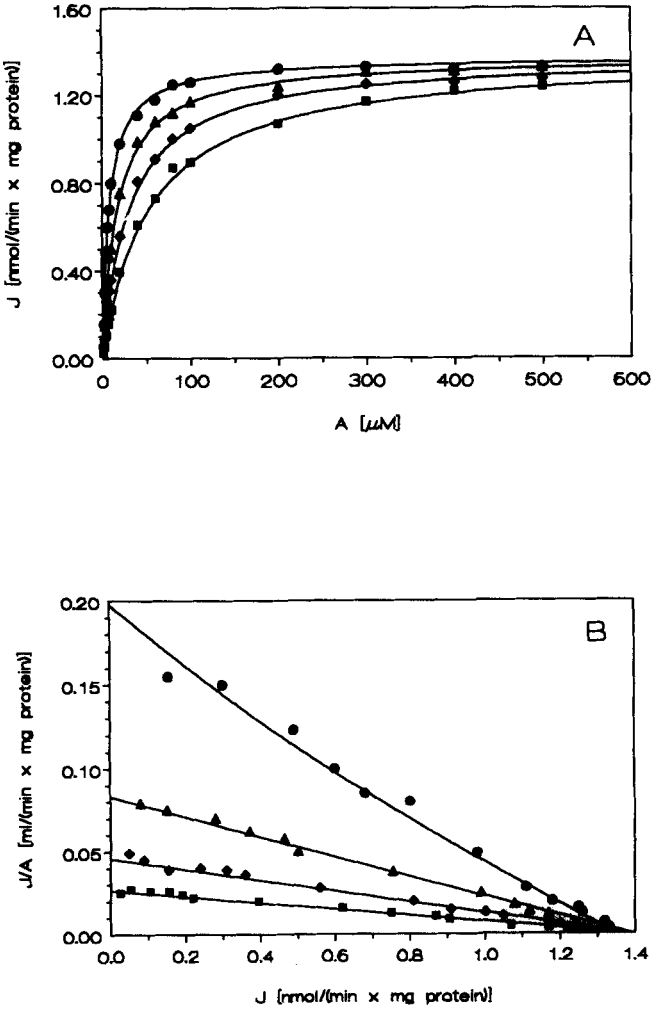

Fig. 10. Effect of different concentrations of SLCT on the dependency of initial flux rates of 7,7-ASLCT into freshly isolated hepatocytes on 7,7-ASLCT concentration in the presence of 143 mM Na^+ (standard medium); (●) in the absence of SLCT, and in the presence of 10 μM (▲), 25 μM (◆), and 50 μM (■) SLCT. A: J-versus-A plot, B: J/A-versus-J plot. The points represent the data of a typical experiment. Curves were calculated applying equations 1 and 3 using the calculated parameters for 7,7-ASLCT and SLCT.

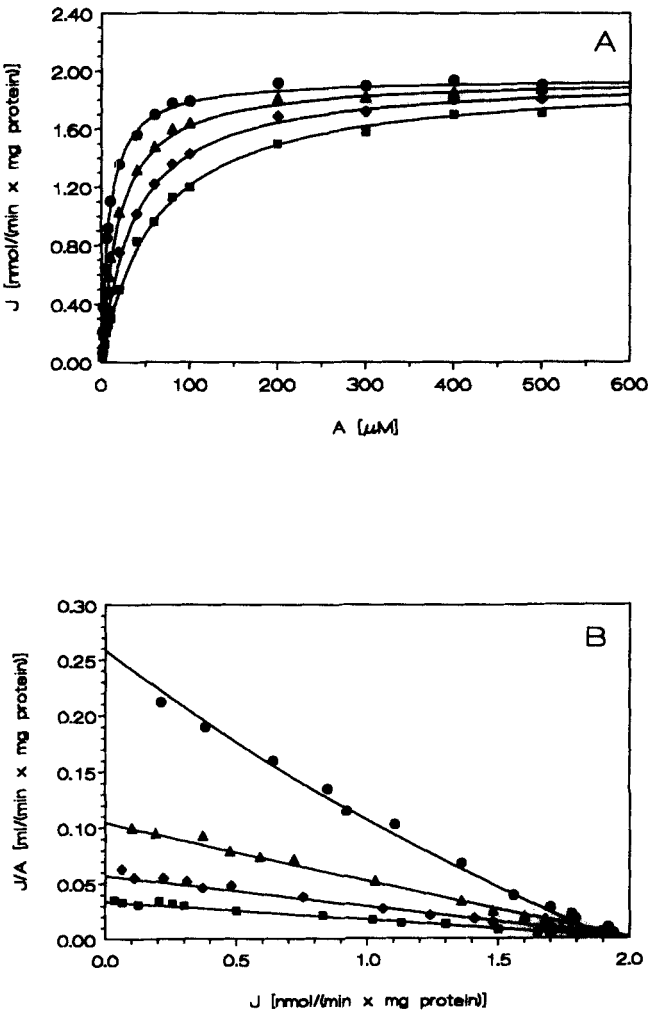

Fig. 11. Effect of different concentrations of 7,7-ASLCT on the dependency of initial flux rates of SLCT into freshly isolated hepatocytes on SLCT concentration in the presence of 143 mM Na^+ (standard medium); (●) in the absence of 7,7-ASLCT, and in the presence of 10 μM (▲), 25 μM (◆), and 50 μM (■) 7,7-ASLCT. A: J-versus-A plot, B: J/A-versus-J plot. The points represent the data of a typical experiment. Curves were calculated applying equations 1 and 3 using the calculated parameters for SLCT and 7,7-ASLCT.

Irreversible inhibition of SLCT uptake by photoaffinity labeling with 7,7-ASLCT

The results of the competition studies were confirmed by the irreversible inhibition of the transport systems

involved in the uptake of sulfated and taurine-conjugated bile salts by photoaffinity labeling of freshly isolated hepatocytes with 400 μM 7,7-ASLCT. In order to avoid any reversible influence of 7,7-ASLCT and its photolytic products on the uptake rate in addition to the irreversible inhibition of transport, subsequent to photoaffinity labeling the noncovalently incorporated bile salts were removed as completely as possible. For this the hepatocytes were repeatedly centrifuged and resuspended, exactly as described (22). As to be expected, photoaffinity labeling of isolated hepatocytes resulted in a clear decrease of the maximal flux rates of both 7,7-ASLCT (data not shown) and SLCT (**Fig. 12**). Irradiation of freshly isolated hepatocytes under the same experimental conditions in the absence of 7,7-ASLCT as one control and incubation of the cells with 400 μM 7,7-ASLCT without irradiation but performing all other experimental steps as alternative control did not practically alter the uptake of 7,7-ASLCT or SLCT. Thus, the decrease of maximal flux rates must be caused by irreversible inhibition of the corresponding transport systems as a result of photoaffinity labeling. The extent of irreversible inhibition of total uptake amounted to about 40% and was within the range of experimental variations the same for 7,7-ASLCT and SLCT. With the assumption that the irreversible inhibition affects only the maximal flux rates and not the half-saturation constants, the K'_T values of the two transport systems for SLCT uptake in the absence of any inhibitor were used for regression analysis applying equation 1. Under the experimental conditions used, maximal flux rate of transport system 1 was reduced to $J'_{1PA} = 0.23$ corresponding to an inhibition by about 60% and that of transport system 2 was lowered to $J'_{2PA} = 0.94$ corresponding to an inhibition by about 30%. Irreversible inhibition of uptake by photoaffinity labeling demonstrates that 7,7-ASLCT and SLCT are taken up into freshly isolated hepatocytes by the same transport systems, and furthermore, that 7,7-ASLCT may be used to trace the uptake of sulfated and taurine-conjugated bile salts.

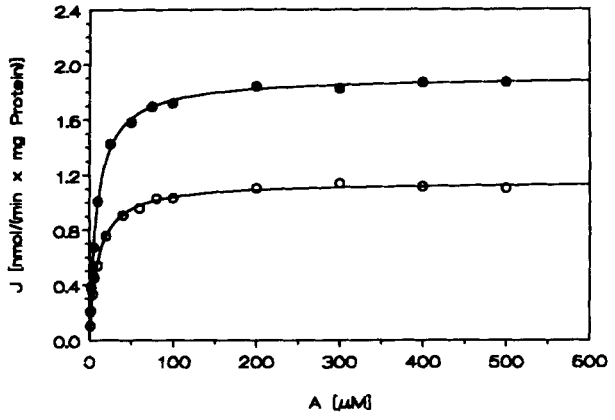

Fig. 12. Effect of photoaffinity labeling of isolated hepatocytes with 7,7-ASLCT on uptake of SLCT. Dependency of initial flux rates of SLCT into isolated hepatocytes on SLCT concentration in 143 mM Na^+ (standard medium); (●) no photoaffinity labeling, and after photoaffinity labeling with (○) 400 μM 7,7-ASLCT. Curves were calculated applying equation 1 using the K'_T values evaluated for SLCT.

Metabolism and excretion of 7,7-ASLCT and SLCT

In order to further evaluate the biological suitability of 7,7-ASLCT for the study of hepatobiliary transport and to receive additional information about the influence of the azi group in position 7 on bile salt transport, infusion experiments were performed with the 3α-sulfated and taurine-conjugated bile salts 7,7-ASLCT, SLCT, and SCCT. Each of the 3α-sulfated and taurine-conjugated bile salts was excreted into bile completely unmetabolized, as scrutinized by HPLC, and in all cases more then 95% of the applied bile salts could be detected in bile within 40 min (**Fig. 13**). In urine, less than 1% of each of the applied compounds was found. The excretion maximum of 7,7-ASLCT was about 5.5 ± 0.8 min, ranging between the values for SCCT and SLCT (**Table 4**). This is an indication that the azi group in position 7 places 7,7-ASLCT according to its excretion behavior between the corresponding methylene and hydroxymethylene derivatives, SLCT and SCCT. However, in the complete course of excretion 7,7-ASLCT and SLCT resembled each other more than SCCT, as became evident by the times needed for the excretion of 50% ($t_{50\%}$) and 90% ($t_{90\%}$) of the applied bile salts (Table 4).

In order to evaluate whether the photolabile derivative is excreted into bile over the path used by SLCT, the inhibition of the biliary maximal excretion rate (T_m) of SLCT by 7,7-ASLCT was investigated. Infusion of increasing concentrations of SLCT led to an increase in its biliary excretion and reached a steady state with the maximal excretion of 130 nmol/(min • 100 g body weight), which is slightly above earlier estimations (49). In accordance with previous investigations (49–51), infusion of the dianionic bile salt did not alter the bile flow. Administration of the small amount of 0.1 μmol of 7,7-ASLCT resulted in a clear decrease of the excretion rate of SLCT (**Fig. 14**). After 7,7-ASLCT had been excreted, excretion of SLCT increased and reached the original rate after about 60 min. This demonstrates that 7,7-ASLCT interferes with the excretion of SLCT and favors the hypothesis that both dianionic bile salts share a common excretion pathway.

In contrast to 7,7-ASLCT, a bolus injection of 0.1 μmol cholyltaurine caused no decrease of the maximal excretion rate of SLCT (Fig. 14), indicating that differ-

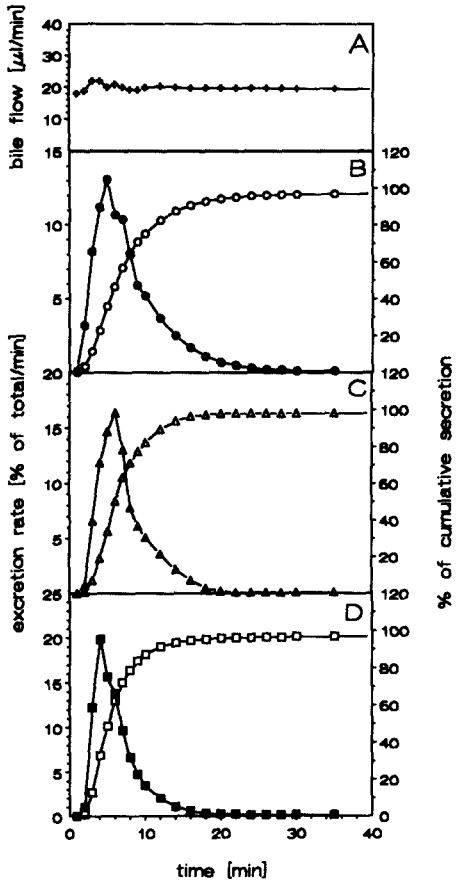

Fig. 13. Time dependency of biliary excretion of sulfated and taurine-conjugated bile salts after a bolus injection of 0.05 nmol of the respective tritium-labeled derivative into a rat mesenterial vein (typical experiment). A: Bile flow (+); B: excretion of [^{3}H]-7,7-ASLCT; C: excretion of [^{3}H]SLCT; D: excretion of [^{3}H]SCCT. The filled symbols show % of dose applied that is excreted in the fraction at the respective time; the open symbols show the cumulative % of radioactivity excreted of total dose injected.

TABLE 4. Biliary excretion of 3α-sulfated and taurine conjugated bile salts

Injected Compound	Excretion		
	t_{max}	$t_{50\%}$	$t_{90\%}$
	min	*min*	*min*
SCCT	4.0 ± 0.3	5.0 ± 0.4	11.2 ± 0.6
7,7-ASLCT	5.5 ± 0.8	7.2 ± 1.5	16.6 ± 4.5
SLCT	6.3 ± 1.1	7.2 ± 1.2	15.5 ± 5.5

Tritium-labeled compounds (0.05 nmol) dissolved in 500 µl of 0.15 M NaCl, pH 7.4, were infused into a peripheral mesenterial vein of anesthetized rats. The compounds were infused over a 1-min period. Bile was collected beginning 10 min before the start of injection during the first 20 min in 1-min intervals, during the following 20 min in 2-min intervals, and finally in 5-min intervals. The times indicated in the table are related to the start of the injection. The data are reported as means ± SEM (n = 4).

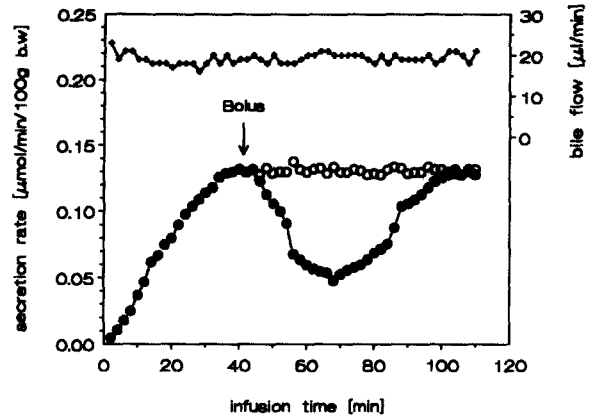

Fig. 14. Bile flow (+) and SLCT excretion in bile during a constant infusion of SLCT (170 nmol/min/100 g b.w.). Injection of an additional bolus of 0.1 µmol of 7,7-ASLCT (●) or cholyltaurine (○) at the time indicated by the arrow. Bile was collected in 2-min intervals.

ent transport systems exist for excretion of dianionic and secretion of monoanionic bile salts.

Suitability of 7,7-ASLCT for biological studies in liver

7,7-ASLCT is intended to be used for eludication of hepatobiliary transport of sulfated and taurine-conjugated bile salts by photoaffinity labeling. In order to be suitable for the planned studies, it is necessary that the photolabile derivative is transported through liver and is excreted into bile just as the corresponding physiological compound SLCT. Therefore, hepatobiliary transport and metabolism of the two dianionic bile salts were compared with each other.

The comparison of the dependency of initial influx rates in the presence of Na^+ and with Na^+ depletion revealed that the photolabile derivative 7,7-ASLCT behaved as the physiological dianionic bile salt SLCT. Uptake of 7,7-ASLCT and SLCT showed a similar Na^+ dependency and both dianionic bile salts were taken up into freshly isolated hepatocytes in the case of Na^+ depletion by two different transport systems. Two transport systems must likewise be operative in the uptake of 7,7-ASLCT and SLCT in the presence of Na^+, as demonstrated by competitive inhibition by cholyltaurine. The competitive inhibition of uptake by cholyltaurine in the presence of Na^+ is similar for 7,7-ASLCT and SLCT, and affects practically only transport system 2 for sulfated and taurine-conjugated bile salts. All kinetic data suggest that the photolabile derivative 7,7-ASLCT behaves in the uptake in isolated hepatocytes like the physiological compound SLCT.

7,7-ASLCT and SLCT show a strictly competitive cross-inhibition in the presence of Na^+ which is describable using the corresponding half-saturation constants as inhibition constants. This justifies the conclusion that

7,7-ASLCT and SLCT are transported into hepatocytes as competing substrates by the same two transport systems. The conclusion drawn is evidenced by irreversible inhibition of the uptake of sulfated and taurine-conjugated bile salts after photoaffinity labeling of freshly isolated hepatocytes using 7,7-ASLCT.

Both dianionic bile salts, 7,7-ASLCT and SLCT, were completely excreted unmetabolized with about the same excretion maximum. Biliary excretion of SLCT was inhibited by 7,7-ASLCT, but was not altered by the presence of cholyltaurine. These findings are in agreement with the conclusion that 7,7-ASLCT and SLCT share a common excreting pathway, differing from that for the monoanionic bile salt cholyltaurine.

Regardless of whether detailed transport mechanisms are operative in the hepatic uptake and the excretion of sulfated and taurine-conjugated bile salts, 7,7-ASLCT has been shown to be, in all respects, a competing substrate of SLCT. Thus 7,7-ASLCT is a promising model compound for the study of hepatobiliary transport of 3α-sulfated and taurine-conjugated bile salts with the aid of photoaffinity labeling, allowing the identification of proteins involved in transport (52).

The authors express their gratitude to Dr. D. Hunkler and Dr. J. Wörth from the Institute für Organische Chemie and Biochemie der Universität Freiburg for the ^{1}H-NMR and mass spectra, and to Dr. C. Quiquerez of the Preclinical Research Department of Sandoz Pharma Ltd. for the FAB mass spectra. This investigation was supported by the Deutsche Forschungsgemeinschaft (SFB 154). One of us (A. Dietrich) is indebted to the Fritz-Thyssen-Stiftung for a scholarship.

Manuscript received 22 September 1994 and in revised form 12 April 1995.

REFERENCES

1. Macdonald, I. A., V. D. Bokkenheuser, J. Winter, A. M. McLernon, and E. H. Mosbach. 1983. Degradation of steroids in the human gut. *J. Lipid Res.* **24:** 675–700.
2. Hylemon, P. B. 1985. Metabolism of bile acids in intestinal microflora. *In* Sterols and Bile Acids. H. Danielsson, and J. Sjövall, editors. Elsevier Science Publishers B. V., Amsterdam, New York, Oxford. 331–343.
3. Hofmann, A. F. 1984. Chemistry and enterohepatic circulation of bile acids. *Hepatology.* **4:** 4S–14S.
4. Elliott, W. H. 1985. Metabolism of bile acids in liver and extrahepatic tissues. *In* Sterols and Bile Acids. H. Danielsson, and J. Sjövall, editors. Elsevier Science Publishers B. V., Amsterdam, New York, Oxford. 303–329.
5. Carey, M. C., and M. J. Cahalane. 1988. Enterohepatic circulation. *In* The Liver: Biology and Pathobiology, Second Edition. I. M. Arias, W. B. Jakoby, H. Popper, D. Schachter, and D. A. Shafritz, editors. Raven Press, Ltd., New York. 573–616.
6. Palmer, R. H. 1967. The formation of bile acid sulfates: a new pathway of bile acid metabolism in humans. *Proc. Natl. Acad. Sci. USA.* **58:** 1047–1050.
7. Palmer, R. H., and M. G. Bolt. 1971. Bile acid sulfates. I. Synthesis of lithocholic acid sulfates and their identification in human bile. *J. Lipid Res.* **12:** 671–679.
8. Cowen, A. E., M. G. Korman, A. F. Hofmann, and O. W. Cass. 1975. Metabolism of lithocholate in healthy man. I. Biotransformation and biliary excretion of intravenously administered lithocholate, lithocholylglycine, and their sulfates. *Gastroenterology.* **69:** 59–66.
9. Cowen, A. E., M. G. Korman, A. F. Hofmann, O. W. Cass, and S. B. Coffin. 1975. Metabolism of lithocholate in healthy man. II. Enterohepatic circulation. *Gastroenterology.* **69:** 67–76.
10. Stiehl, A., D. L. Earnest, and W. H. Admirand. 1975. Sulfation and renal excretion of bile salts in patients with cirrhosis of the liver. *Gastroenterology.* **68:** 534–544.
11. Low-Beer, T. S., M. P. Tyor, and L. Lack. 1969. Effects of sulfation of taurolithocholic and glycolithocholic acids on their intestinal transport. *Gastroenterology.* **56:** 721–726.
12. De Witt, E. H., and L. Lack. 1980. Effects of sulfation patterns on intestinal transport of bile salt sulfate esters. *Am. J. Physiol.* **238:** G34–G39.
13. Kuipers, F., H. Heslinga, R. Havinga, and R. J. Vonk. 1986. Intestinal absorption of lithocholic acid sulfates in the rat: inhibitory effects of calcium. *Am. J. Physiol.* **251:** G189–G194.
14. Allan, R. N., J. L. Thistle, A. F. Hofmann, J. A. Carter, and P. Y. S. Yu. 1976. Lithocholate metabolism during chenotherapy for gallstone dissolution. 1. Serum levels of sulphated and unsulphated lithocholates. *Gut.* **17:** 405–412.
15. Allan, R. N., J. L. Thistle, and A. F. Hofmann. 1976. Lithocholate metabolism during chenotherapy for gallstone dissolution. 2. Absorption and sulphation. *Gut.* **17:** 413–419.
16. Hofmann, A. F. 1988. Bile acids. *In* The Liver: Biology and Pathobiology, Second Edition. I. M. Arias, W. B. Jakoby, H. Popper, D. Schachter, and D. A. Shafritz, editors. Raven Press, Ltd., New York. 553–572.
17. Palmer, R. H. 1971. Bile acid sulfates. II. Formation, metabolism, and excretion of lithocholic acid sulfates in the rat. *J. Lipid Res.* **12:** 680–687.
18. Bartholomew, T. C., and B. H. Billing. 1983. The effect of 3-sulphation and taurine conjugation on the uptake of chenodeoxycholic acid by rat hepatocytes. *Biochim. Biophys. Acta.* **754:** 101–109.
19. Kuipers, F., R. Havinga, and R. J. Vonk. 1985. Cholestasis induced by sulphated glycolithocholic acid in the rat: protection by endogenous bile acids. *Clin. Sci.* **68:** 127–134.
20. Takikawa, H., J. Tomita, T. Takemura, and M. Yamanaka. 1991. Cytotoxic effect and uptake mechanism by isolated rat hepatocytes of lithocholate and its glucuronide and sulfate. *Biochim. Biophys. Acta.* **1091:** 173–178.
21. Fricker, G., S. Schneider, W. Gerok, and G. Kurz. 1987. Identification of different transport systems for bile salts in sinusoidal and canalicular membranes of hepatocytes. *Biol. Chem. Hoppe-Seyler.* **368:** 1143–1150.
22. Schramm, U., G. Fricker, H-P. Buscher, W. Gerok, and G. Kurz. 1993. Fluorescent derivatives of bile salts. III. Uptake of 7β-NBD-NCT into isolated hepatocytes by the transport systems for cholyltaurine. *J. Lipid Res.* **34:** 741–757.

23. Paumgartner, G., K. Sauter, H. P. Schwarz, and R. Herz. 1973. Hepatic excretory transport maximum for free and conjugated cholate in the rat. *In* The Liver. Quantitative Aspects of Structure and Function. Karger, Basel, Switzerland. 337–344.
24. Berry, M. N., and D. S. Friend. 1969. High-yield preparation of isolated rat liver parenchymal cells. A biochemical and fine structural study. *J. Cell. Biol.* **43:** 506–520.
25. Seglen, P. O. 1976. Preparation of isolated rat liver cells. *Methods Cell. Biol.* **13:** 29–83.
26. Berry, M. N., A. M. Edwards, G. J. Barritt, M. B. Grivell, H. J. Halls, B. J. Gannon, and D. S. Friend. 1991. Isolated hepatocytes. Preparation, properties and applications. *In* Laboratory Techniques in Biochemistry and Molecular Biology. Vol. 21. R. H. Burdon and P. H. van Knippenberg, editors. Elsevier, Amsterdam, New York, Oxford.
27. Page, R. A., K. M. Stowell, M. J. Hardman, and K. E. Kitson. 1992. The assessment of viability in isolated rat hepatocytes. *Anal. Biochem.* **200:** 171–175.
28. Kramer, W., U. Bickel, H-P. Buscher, W. Gerok, and G. Kurz. 1982. Bile-salt-binding polypeptides in plasma membranes of hepatocytes revealed by photoaffinity labelling. *Eur. J. Biochem.* **129:** 13–24.
29. Laemmli, U. K. 1970. Cleavage of structural proteins during the assembly of the head of bacteriophage T4. *Nature.* **227:** 680–685.
30. Hübscher, G., G. R. West, and D. N. Brindley. 1965. Studies on the fractionation of mucosal homogenates from the small intestine. *Biochem. J.* **97:** 629–642.
31. Makino, I., and J. Sjövall. 1972. A versatile method for analysis of bile acids in plasma. *Anal. Lett.* **5:** 341–349.
32. Still, W. C., M. Kahn, and A. Mitra. 1978. Rapid chromatographic technique for preparative separations with moderate resolution. *J. Org. Chem.* **43:** 2923–2925.
33. Rossi, S. S., J. L. Converse, and A. F. Hofmann. 1987. High pressure liquid chromatographic analysis of conjugated bile acids in human bile: simultaneous resolution of sulfated and unsulfated lithocholyl amidates and the common conjugated bile acids. *J. Lipid Res.* **28:** 589–595.
34. Lawson, A. M., and K. D. R. Setchell. 1988. Mass spectrometry of bile acids. *In* The Bile Acids. Chemistry, Physiology, and Metabolism. Volume 4. K. D. R. Setchell, D. Kritchevsky, and P. P. Nair, editors. Plenum Press, New York, London. 167–267.
35. Lawson, A. M. 1989. Mass spectrometry—the fundamental principles. *In* Mass Spectrometry. A. M. Lawson, editor. Walter de Gruyter, Berlin, New York. 1–52.
36. Setchell, K. D. R., and A. M. Lawson. 1989. Bile acids. *In* Mass Spectrometry. A. M. Lawson, editor. Walter de Gruyter, Berlin, New York. 53–125.
37. Fieser, L. F., and S. Rajagopalan. 1950. Oxidation of steroids. III. Selective oxidations and acylations in the bile acid series. *J. Am. Chem. Soc.* **72:** 5530–5536.
38. Kramer, W., and G. Kurz. 1983. Photolabile derivatives of bile salts. Synthesis and suitability for photoaffinity labeling. *J. Lipid Res.* **24:** 910–923.
39. Tserng, K-Y., and P. D. Klein. 1977. Synthesis of sulfate esters of lithocholic acid, glycolithocholic acid, and taurolithocholic acid with sulfur trioxide-triethylamine. *J. Lipid Res.* **18:** 491–495.
40. Mosbach, E. H., W. Meyer, and F. E. Kendall. 1954. Preparation and $NaBH_4$ reduction of 7-ketocholanic acid. *J. Am. Chem. Soc.* **76:** 5799–5801.
41. Parmentier, G., and H. Eyssen. 1977. Synthesis and characteristics of the specific monosulfates of chenodeoxycholate, deoxycholate and their taurine or glycine conjugates. *Steroids.* **30:** 583–590.
42. Goto, J., H. Kato, F. Hasegawa, and T. Nambara. 1979. Synthesis of monosulfates of unconjugated and conjugated bile acids. *Chem. Pharm. Bull.* **27:** 1402–1411.
43. Tang, P. W., and D. L. Crone. 1989. A new method for hydrolyzing sulfate and glucuronyl conjugates of steroids. *Anal. Biochem.* **182:** 289–294.
44. Dayal, B., G. Salen, B. Toome, G. S. Tint, S. Shefer, and J. Padia. 1990. Lithium hydroxide/aqueous methanol: mild reagent for the hydrolysis of bile acid methyl esters. *Steroids.* **55:** 233–237.
45. Une, M., F. Nagai, and T. Hoshita. 1983. High-performance liquid chromatographic separation of higher bile acids. *J. Chromatogr.* **257:** 411–415.
46. Gengenbacher, T., W. Gerok, U. Giese, and G. Kurz. 1990. Synthesis and applicability of photolabile 7,7-azo analogues of natural bile salt precursors. *J. Lipid Res.* **31:** 315–327.
47. Stoll, G. H., R. Voges, W. Gerok, and G. Kurz. 1991. Synthesis of a metabolically stable modified long-chain fatty acid salt and its photolabile derivative. *J. Lipid Res.* **32:** 843–857.
48. Gerok, W., G. Kurz, and D. Schwab. 1994. Transport of conjugated and unconjugated bile salts across the sinusoidal membrane. *In* Transport in the Liver. D. Keppler and K. Jungermann, editors. Kluwer Academic Publishers, Lancaster, England. 82–94.
49. Mathis, U., G. Karlaganis, and R. Preisig. 1983. Monohydroxy bile salt sulfates: Tauro-3β-hydroxy-5-cholenoate-3-sulfate induces intrahepatic cholestasis in rats. *Gastroenterology.* **85:** 674–681.
50. Yousef, I. M., B. Tuchweber, R. J. Vonk, D. Masse, M. Audet, and C. C. Roy. 1981. Lithocholate cholestasis—sulfated glycolithocholate-induced intrahepatic cholestasis in rats. *Gastroenterology.* **80:** 233–241.
51. van der Meer, R., R. J. Vonk, and F. Kuipers. 1988. Cholestasis and the interactions of sulfated glyco- and taurolithocholate with calcium. *Am. J. Physiol.* **254:** G644–G649.
52. Dietrich, A., W. Dieminger, K. Fuchte, G. H. Stoll, W. Gerok, and G. Kurz. 1995. Functional significance of interaction of H-FABP with sulfated and nonsulfated taurine conjugated bile salts in rat liver. *J. Lipid Res.* **36:** 1745–1755.